

AD-A047 288

NAVAL UNDERWATER SYSTEMS CENTER NEW LONDON CONN NEW --ETC F/G 20/14
SCATTERING OF PLANE WAVES FROM A COMPLIANT TUBE GRATING IN A LI--ETC(U)
AUG 77 R P RADLINSKI
NUSC-TR-5433

UNCLASSIFIED

[OF]
AD
A047288

NL



AD A 0 4 7 2 8 8

NUSC Technical Report 5433

⁹ NUSC Technical Report 5433

¹⁴ NUSC -TR-5433



¹² B.S.

⁶ Scattering of
Plane Waves from a
Compliant Tube Grating in a
Linear Viscoelastic Layer.

¹⁶

F11121

¹⁰ Ronald P. Radlinski
Special Projects Department

¹⁷

SF11121702

DDC
RECEIVED
DEC 6 1977
RECEIVED
D

¹¹ 18 Aug 1977

¹³ 38p.

NUSC

NAVAL UNDERWATER SYSTEMS CENTER
Newport, Rhode Island • New London, Connecticut

Approved for public release; distribution unlimited.

AD No. _____

DDC FILE COPY

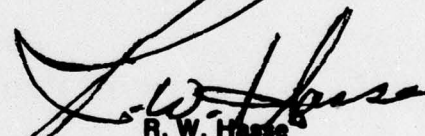
405 918

PREFACE

This investigation was supported by NUSC Project No. A-700-11, "Large Aperture Array Development," Principal Investigator, J. J. Libuha (Code 316), and Navy Subproject and Task No. SF 11 121702 16727, Program Manager, C. C. Walker, Naval Sea Systems Command (Code 06H1-2).

The Technical Reviewer for this report was H. L. Pond (Code 316).

REVIEWED AND APPROVED: 18 August 1977



R. W. Hasse
Head: Special Projects Department

The author of this report is located at the New London Laboratory, Naval Underwater Systems Center, New London, Connecticut 06320.

REPORT DOCUMENTATION PAGE		READ INSTRUCTIONS BEFORE COMPLETING FORM
1. REPORT NUMBER TR 5433	2. GOVT ACCESSION NO.	3. RECIPIENT'S CATALOG NUMBER
4. TITLE (and Subtitle) SCATTERING OF PLANE WAVES FROM A COMPLIANT TUBE GRATING IN A LINEAR VISCOELASTIC LAYER		5. TYPE OF REPORT & PERIOD COVERED
7. AUTHOR(s) Ronald P. Radlinski		6. PERFORMING ORG. REPORT NUMBER
9. PERFORMING ORGANIZATION NAME AND ADDRESS Naval Underwater Systems Center New London Laboratory New London, CT 06320		8. CONTRACT OR GRANT NUMBER(s)
11. CONTROLLING OFFICE NAME AND ADDRESS Naval Sea Systems Command (SEA 06H1-2) Washington, DC 20362		10. PROGRAM ELEMENT, PROJECT, TASK AREA & WORK UNIT NUMBERS A70011 SF 11 121702 16727
14. MONITORING AGENCY NAME & ADDRESS (if different from Controlling Office)		12. REPORT DATE 18 August 1977
		13. NUMBER OF PAGES 32
		15. SECURITY CLASS. (of this report) UNCLASSIFIED
		15a. DECLASSIFICATION/DOWNGRADING SCHEDULE
16. DISTRIBUTION STATEMENT (of this Report) Approved for public release; distribution unlimited.		
17. DISTRIBUTION STATEMENT (of the abstract in Block 20, if different from Report)		
18. SUPPLEMENTARY NOTES		
19. KEY WORDS (Continue on reverse side if necessary and identify by block number) Viscoelastic Layer Multiple Scattering Shear Waves Planar Resonant Compliant Tube Gratings Reflective Baffles		
20. ABSTRACT (Continue on reverse side if necessary and identify by block number) The nature of plane wave scattering from a grating in a viscoelastic medium is shown to be fundamentally different from that in a fluid or elastic medium. The solution to the generalized Helmholtz equation is determined in terms of inhomogeneous plane dilatational or shear (P or S) waves. Angles between the propagating and attenuating wave vectors are determined by the boundary conditions. The evanescent waves that arise from the grating equations cannot propagate parallel to the grating as is the case for an elastic-like or fluid medium. Measured transmission loss		

20. (cont'd)

of plane waves incident on a compliant tube layer in a fluid are compared with predictions of an analytical model. The effects of the elastic stiffness and the mechanical loss factors of a layer of linear viscoelastic material on the performance of the compliant tube arrays are investigated for two different elastomeric encapsulants. Values of the complex shear modulus used as input to the model were determined by use of viscoelastic temperature-frequency relationships.

TABLE OF CONTENTS

	Page
LIST OF ILLUSTRATIONS	ii
INTRODUCTION	1
MATHEMATICAL FORMULATION	2
Description of the Problem	2
Grating in a Linear Viscoelastic Medium	2
Analytical Description of Compliant Tubes	7
Description of Compliant Tube Grating in a Thin Visco- elastic Layer Immersed in a Fluid.	12
Boundary Conditions and Infinite System of Equations . .	15
COMPARISON OF CALCULATIONS AND EXPERIMENTAL DATA	23
Experimental Procedure	23
Insertion Loss	23
CONCLUSIONS	26
REFERENCES	31

ACCESSION for	
NTIS	White Section <input checked="" type="checkbox"/>
DDC	Buff Section <input type="checkbox"/>
UNANNOUNCED	<input type="checkbox"/>
JUSTIFICATION.....	
BY.....	
DISTRIBUTION/AVAILABILITY CODES	
Dist.	AVAIL. and/or SPECIAL
A	

DDC
RECEIVED
 DEC 6 1977
RECEIVED
 D

LIST OF ILLUSTRATIONS

Figure		Page
1	Plane Wave Normally Incident on an Encapsulated Grating of Compliant Tubes in a Fluid	3
2	Deflection Shape of the Lowest Membrane and Two Lowest Bending Modes of a Compliant Shell	8
3	Fundamental Bending Waveform of an Elliptic Ring	11
4	Plastic Tube Encapsulated in Polyurethane	24
5	Comparison of Calculation and Measurement of Insertion Loss for 0.375 in. (9.52 mm) Lexan Plastic Tubes in a 0.45 in. (11.50 mm) Spaced Grating Encapsulated with a 0.5 in. (12.7 mm) Layer of Low Shear Modulus Rubber . . .	25
6	Comparison of Calculation and Measurement of Insertion Loss for 0.375 in. (9.52 mm) Lexan Plastic Tubes in a 0.45 in. (11.50 mm) Spaced Grating Encapsulated with a 0.5 in. (12.7 mm) Layer of Polyurethane	27
7	Comparison of Calculation and Measurement of Insertion Loss for 0.925 in. (23.50 mm) Steel Compliant Tubes in a 1 in. (25.4 mm) Spaced Grating Encapsulated with a 1 in. (25.4 mm) Thick Layer of Low Shear Modulus Rubber .	28
8	Comparison of Calculation and Measurement of Insertion Loss for 0.925 in. (23.5 mm) Steel Compliant Tubes in a 1 in. (25.4 mm) Spaced Grating Encapsulated with a 1 in. (25.4 mm) Thick Layer of Polyurethane	29

SCATTERING OF PLANE WAVES FROM A COMPLIANT TUBE GRATING IN A LINEAR VISCOELASTIC LAYER

INTRODUCTION

The use of compliant tubes as a reflector in a fluid medium has been studied both experimentally and analytically by Toulis,¹ and more recently by investigators at the Naval Underwater Systems Center (NUSC).^{2,3} The latter work has shown that through the use of multiple-layered, compliant tube baffles of wide and tunable bandwidths of reflectivity can be achieved. Brigham and Radlinski⁴⁻⁶ have developed an analytical model of scattering plane waves from an infinitely wide array of elliptical shells in a fluid medium. The calculations from this model agree with the experimental transmission measurements from both plastic and steel compliant tube arrays. Brigham⁷ has extended the above model to include scattering from planar compliant tube arrays in an infinite elastic medium.

In this report, the scattering of a plane wave from a planar grating of compliant tubes embedded in a linear viscoelastic layer is analyzed through the use of an approximate solution. In the formulation, the tubes are treated as rectangular elements. Only the case where the tubes are aligned perpendicular to the direction of the plane wave that is normally incident to the grating is considered here. The reason for these limitations is the severe mathematical complexity of analyzing inclusions of arbitrary shape and orientation in a plane layer. Since the range of frequency has been extended from the previous works, higher order structural modes are important to the analysis. The solution in the viscoelastic layer is given in terms of inhomogeneous plane waves (that is, a wave that is attenuated along the lines of constant phase). The periodic nature of the solution makes it possible to reduce a continuous angular spectrum of plane waves to a discrete number of propagating and exponentially decaying waves.

To obtain the necessary material parameters as input for the analytical models, the elastic Young's modulus and mechanical loss factors were measured in the 100 Hz to 2 kHz frequency range using the Brüel and Kjaer complex Young's modulus apparatus. The temperature-frequency scaling relationships were applied to the measured data to calculate the elastic modulus in the frequency range of interest.⁸ Since longitudinal velocities of these materials have a relatively small variation with frequency and temperature, measurements at a single temperature and frequency as reported by other investigators⁹ were used for the study.

Of specific interest is the effect of the elastomeric stiffness on the compliant tube array resonance frequency and the amount of absorption for a given mechanical loss factor of the elastomer. The dynamic compliance of an individual tube in the array is also a parameter that strongly affects the transmission and reflection from the grating. Comparisons of the experimental measurements and the predictions of the model are given for broad frequency spectra and wide ranges of material constants. However, they are not meant to include all measurements made at this time, but rather to illustrate the capabilities of the analytical model.

MATHEMATICAL FORMULATION

DESCRIPTION OF THE PROBLEM

This study concerns the scattering of a plane wave incident through a fluid medium on to a planar grating of compliant tubes embedded in a viscoelastic layer. In particular, insertion loss is calculated for a plane wave normally incident on the layer in a fluid as shown in figure 1.

GRATING IN A LINEAR VISCOELASTIC MEDIUM

In a linear viscoelastic medium, the three-dimensional wave equation can be written as

$$(\lambda + 2\mu)\vec{\nabla}\Delta - \mu\vec{\nabla} \times (2\vec{\omega}) = \rho \frac{\partial^2 \vec{u}}{\partial t^2} \quad (1)$$

where λ and μ are the frequency dependent, complex valued, material properties that reduce to the Lamé constants in the limiting elastic case. The symbol \vec{u} is the displacement vector, $\Delta = \vec{\nabla} \cdot \vec{u}$ is the dilatation, $2\vec{\omega} = \vec{\nabla} \times \vec{u}$ is the rotation, and ρ is the density of the viscoelastic medium. This formulation is equivalent to the Kelvin-Voigt model with harmonic time dependence assumed. The solution to (1) can be found by using a theorem given by Helmholtz which states that there exists a scalar potential ϕ and a vector potential \vec{A} such that the displacement field may be expressed as

$$\vec{u} = \vec{\nabla}\phi + \vec{\nabla} \times \vec{A}, \quad (2a)$$

where

$$\vec{\nabla} \cdot \vec{A} = 0. \quad (2b)$$

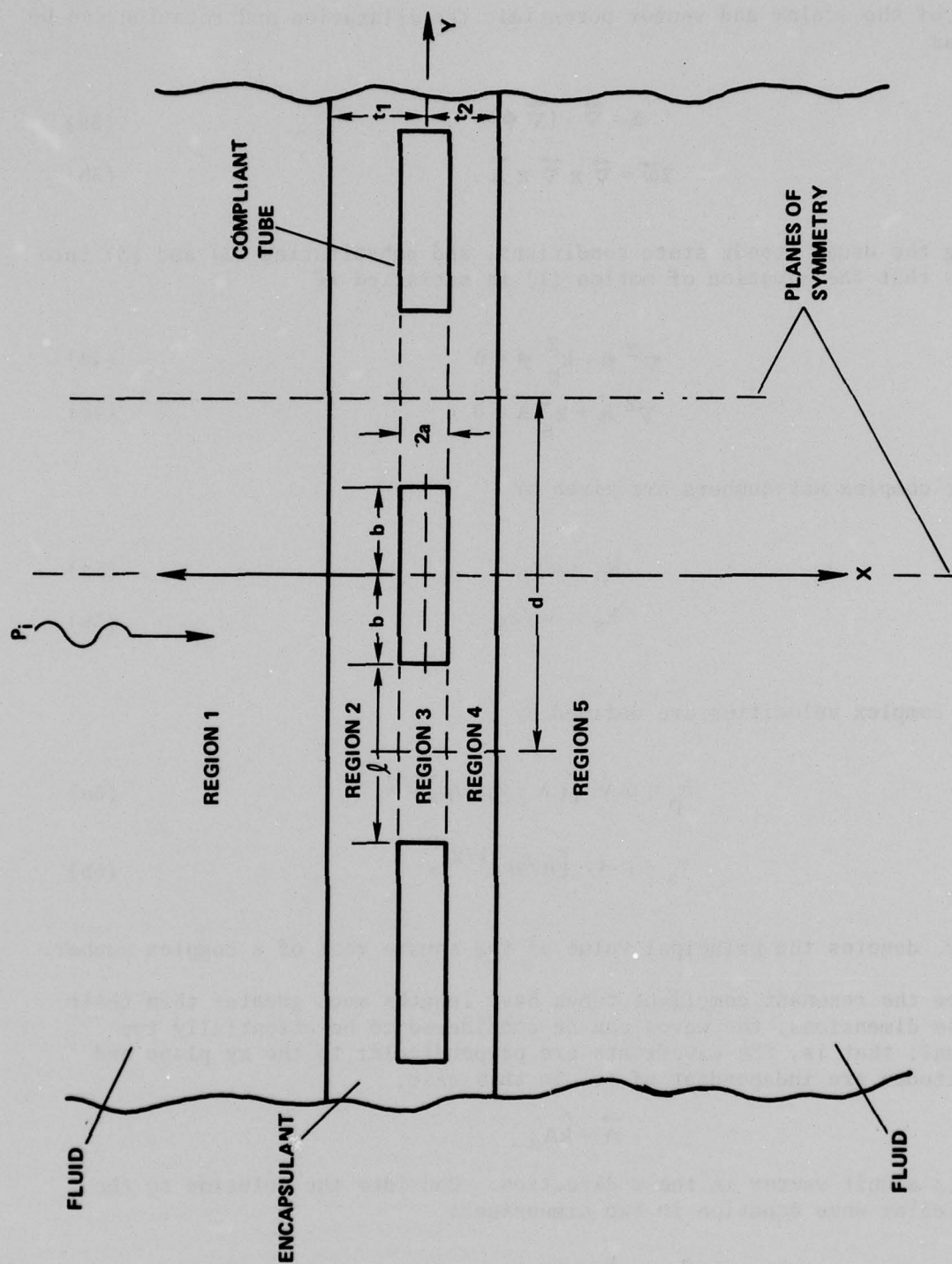


Figure 1. Plane Wave Normally Incident on an Encapsulated Grating of Compliant Tubes in a Fluid

In terms of the scalar and vector potential, the dilatation and rotation can be written as

$$\Delta = \vec{\nabla} \cdot (\vec{\nabla} \phi) \quad (3a)$$

$$2\vec{\omega} = \vec{\nabla} \times \vec{\nabla} \times \vec{A}. \quad (3b)$$

Employing the usual steady state conditions, and substituting (2) and (3) into (1) shows that the equation of motion (1) is satisfied if

$$\nabla^2 \phi + k_p^2 \phi = 0 \quad (4a)$$

$$\nabla^2 \vec{A} + k_s^2 \vec{A} = 0, \quad (4b)$$

where the complex wavenumbers are given by

$$k_p = \omega/c_p \quad (5a)$$

$$k_s = \omega/c_s. \quad (5b)$$

Here the complex velocities are defined by

$$c_p = \text{p.v.} [(\lambda + 2\mu)/\rho]^{1/2} \quad (6a)$$

$$c_s = \text{p.v.} [\mu/\rho]^{1/2}, \quad (6b)$$

where p.v. denotes the principal value of the square root of a complex number.

Since the resonant compliant tubes have lengths much greater than their transverse dimensions, the waves can be considered to be essentially two dimensional; that is, the wavefronts are perpendicular to the xy plane and the amplitudes are independent of z. In this case,

$$\vec{A} = \hat{k} A_z,$$

where \hat{k} is a unit vector in the z direction. Consider the solution to the general scalar wave equation in two dimensions:

$$\left(\frac{\partial^2}{\partial x^2} + \frac{\partial^2}{\partial y^2} \right) \xi + k^2 \xi = 0, \quad (7)$$

where k is the complex wavenumber. Separation of variables implies that the general solution of (7) for an assumed steady state condition is a general plane wave of the form

$$\xi = \xi_0 e^{i\vec{P} \cdot \vec{r}} e^{-\vec{Q} \cdot \vec{r}}, \quad (8a)$$

where P is the propagation vector and Q is the attenuation vector or

$$\xi = \xi_0 e^{i(P_x + iQ_x)x} e^{i(P_y + iQ_y)y}. \quad (8b)$$

Substitution of (8b) into (7) yields

$$k^2 = (P_x + iQ_x)^2 + (P_y + iQ_y)^2. \quad (9a)$$

Now, let

$$k_x = (P_x + iQ_x) \quad (9b)$$

$$k_y = (P_y + iQ_y); \quad (9c)$$

then

$$k_x = \text{p.v. } (k^2 - k_y^2)^{1/2}. \quad (9d)$$

In general, the components of the propagation and attenuation vectors must be determined by the boundary conditions. In the cases under consideration where the compliant tubes are arranged in a planar grating, which for computational purposes is assumed infinite in extent along the y -axis, these vector directions are readily determined.

If the solution is periodic in y , then (for normally incident waves)

$$\xi(x, y) = \xi(x, y+d), \quad (10)$$

where d is the periodic grating spacing. Substitution of (8b) into (10) leads to the condition

$$e^{iP_y d} e^{-Q_y d} = 1, \quad (11a)$$

which implies

$$P_y d = 2\pi n; \quad (11b)$$

and thus,

$$Q_y = 0$$

$$Q_x = \pm Q. \quad (11c)$$

The sign of Q_x will be chosen such that the wave decays as it travels through the viscoelastic medium.

Now from (8) and (9), the general periodic solution of the potential for normally incident waves has the form

$$\begin{aligned} \xi(x, y, t) &= \sum_{n=-\infty}^{\infty} e^{i \left\{ \text{p.v.} \left[k^2 - \left(\frac{2\pi n}{d} \right)^2 \right]^{1/2} \right\} x} e^{i \left(\frac{2\pi n}{d} \right) y} e^{i\omega t} \\ &= \sum_{n=-\infty}^{\infty} e^{i \left\{ \text{Re p.v.} \left[k^2 - \left(\frac{2\pi n}{d} \right)^2 \right]^{1/2} x + \left(\frac{2\pi n}{d} \right) y \right\}} \\ &\quad \times e^{-\text{Im} \left\{ \text{p.v.} \left[k^2 - \left(\frac{2\pi n}{d} \right)^2 \right]^{1/2} \right\} x} e^{i\omega t}. \end{aligned} \quad (12)$$

From (12), one sees that the attenuation is always in a direction normal to the plane of the grating. When

$$\text{Re } k^2 \geq \left(\frac{2\pi n}{d} \right)^2, \quad (13a)$$

the waves are propagating waves whose direction is determined by the order n . For n equal to zero, the direction of propagation and attenuation is the same. For other values of n , the amplitude of the wave varies along the wavefront.

The waves for which

$$\text{Re } k^2 < \left(\frac{2\pi n}{d} \right)^2 \quad (13b)$$

are referred to in the elastic or fluid medium as the evanescent modes for which the waves propagate along the grating and decay exponentially normal to the grating. As seen in (12), the attenuation of evanescent waves in a linear viscoelastic medium is normal to the grating; thus, the propagation necessarily cannot be normal to the attenuation and is the only wave that cannot propagate. For more complete treatises on linear viscoelastic media, consult the works of Cooper,¹⁰ Cooper and Reiss,¹¹ Buchen,¹² and Borchardt.^{13,14}

Assuming plain strain conditions, the normal and tangential deflections are calculated from scalar and vector potentials as

$$\vec{u} = \vec{\nabla} \phi + \vec{\nabla} \times \vec{A}; \quad (14a)$$

then

$$u_x = \frac{\partial \phi}{\partial x} + \frac{\partial A_z}{\partial y} \quad (14b)$$

$$u_y = \frac{\partial \phi}{\partial y} - \frac{\partial A_z}{\partial x}. \quad (14c)$$

The stress is calculated from

$$\sigma_{ij} = \lambda \Delta \delta_{ij} + \mu \left(\frac{\partial u_i}{\partial x_j} + \frac{\partial u_j}{\partial x_i} \right), \quad (15)$$

where the Kronecker delta δ is defined as

$$\delta_{ij} = 1 \quad i = j$$

$$\delta_{ij} = 0 \quad i \neq j,$$

and the dilatation Δ is given by

$$\Delta = \frac{\partial u_x}{\partial x} + \frac{\partial u_y}{\partial y}.$$

ANALYTICAL DESCRIPTION OF COMPLIANT TUBES

Usually described as a long oval shell, deflection profiles for bending and membrane modes of a compliant tube are exemplified in figure 2. As shown in an analysis by Toulis¹ and confirmed at NUSC,³ the frequency and waveform of the fundamental even bending mode of a compliant tube can be estimated by the first bending mode of a clamped-clamped beam.

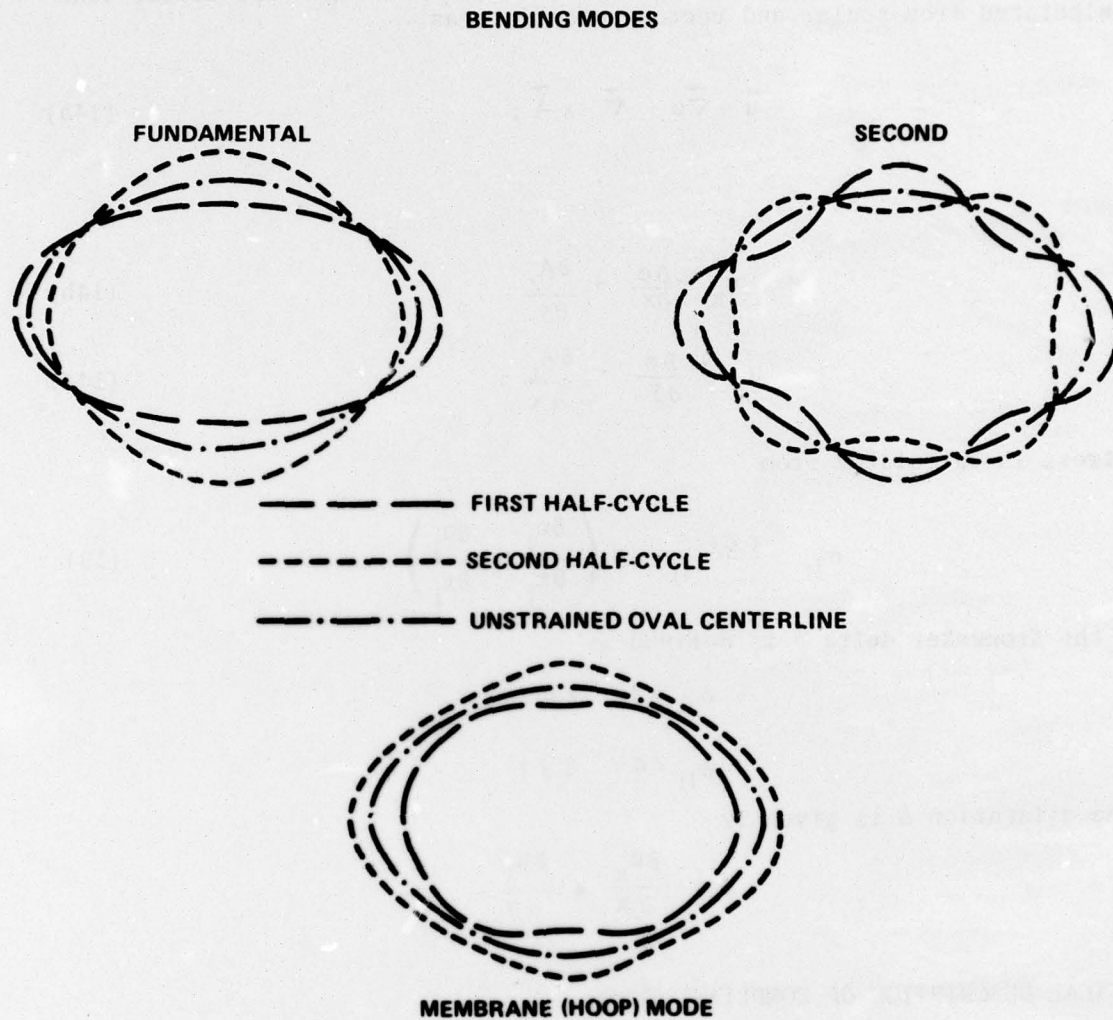


Figure 2. Deflection Shape of the Lowest Membrane and Two Lowest Bending Modes of a Compliant Shell

In the present formulation, the compliant tube is treated acoustically as long thin rectangular plates of width $2b$ with rigid connections of width $2a$, but is modified structurally to account for the decreased compliance with decreased eccentricity. Since only plane waves normally incident to the grating are considered here, only modes symmetric about the x -axis are excited.

At the surface of the compliant tube, normal stress, tangential shearing stress, and radial and tangential displacements are continuous for bonded elastomers. For thin-walled tubes and small displacements, the stress boundary conditions are equivalent to radial and tangential force equations defined in terms of the shell displacements.⁷ All stresses are taken at the mid-surface of the shell. For certain conditions, the shell equations for the compliant tube can be decoupled. At low frequencies where only bending is important, the inextensional condition can be used to derive a single differential force equation relating the normal deflections to the external stresses. To obtain the membrane modes, a single differential equation results by assuming that the motion is primarily radial and thus setting tangential displacement to zero and neglecting bending terms. Furthermore, for thin walled cylinders, the effect of the tangential shearing stress is much smaller than the normal stress. A simplified equation for the normal bending is given by the plate equation

$$\frac{Eh_s^3}{12(1-\nu^2)} \frac{d^4 V}{dy^4} - \omega^2 \rho_s h_s V = \sigma_{xx}, \quad (16)$$

where σ_{xx} is the applied normal stress, V is the normal displacement, E is the Young's modulus of the shell material, h_s is the shell thickness, ρ_s is the shell density, and ν is Poisson's ratio.⁵ The rigid body motion is found by simply setting E to zero. The above equation for bending is further simplified by use of the normal modes defined for the homogeneous form of equation (16) such that

$$\rho_s h_s \sum_t \omega_t^2 V_t \psi_t = \frac{Eh_s^3}{12(1-\nu^2)} \sum_t V_t \frac{d^4 \psi_t}{dy^4} \quad (17)$$

and

$$V = \sum_t V_t \psi_t,$$

where ψ_t is the eigenfunction of the normal bending mode with the corresponding amplitude V_t . ω_t is the resonance frequency of the t -th normal mode. By using (16), a small correction to the effective inertia of the shell wall has been neglected for eccentricities not equal to one.⁷

The fundamental bending mode reflection profile for a clamped-clamped beam of length $2b$ is taken as

$$\psi_2 = Ne_2 \left(1 - \frac{y^2}{2b^2}\right) \quad -b \leq y \leq b. \quad (18)$$

Here, Ne_2 is the normalization constant calculated from the condition

$$\int_{-b}^b |\psi_2|^2 dy = b, \quad (19)$$

which results in $Ne_2 = 1.11$. For compliant tube eccentricities that are small compared with 1, the deflection profiles of an elliptical ring as given by Brigham¹⁵ are used for ψ_n . The deflection profiles for the fundamental even-even bending mode for various values of ratio a/b are shown in figure 3. As a/b approaches one, the net deflection approaches zero, and the tubes become less compliant. Either a Fourier series fit or least squares fit to the deflection profile is used. Higher order bending modes that are resonant in the frequency range are also included in the analysis. The rigid body wave function to a first approximation is a constant which is normalized as above.

For plastic compliant tubes, the fundamental membrane mode is important to the analysis, since it becomes resonant in the frequency range of interest. The eigenvalues and eigenfunctions of the fundamental membrane mode of uniformly thick elliptical shells have also been determined by Brigham.¹⁶ The resonance frequency of the fundamental membrane mode is given by

$$\omega_1 \approx \frac{\pi c_s}{2S_0} = \frac{\pi[E/\rho(1-\nu^2)]^{1/2}}{2S_0}. \quad (20)$$

Here, c_s is the speed of sound in the compliant tube material and S_0 is defined by the elliptic integral

$$S_0 = b \int_0^\pi [1 - e^2 \sin^2 \phi]^{1/2} d\phi, \quad (21)$$

where e is the eccentricity

$$e^2 = 1 - a^2/b^2.$$

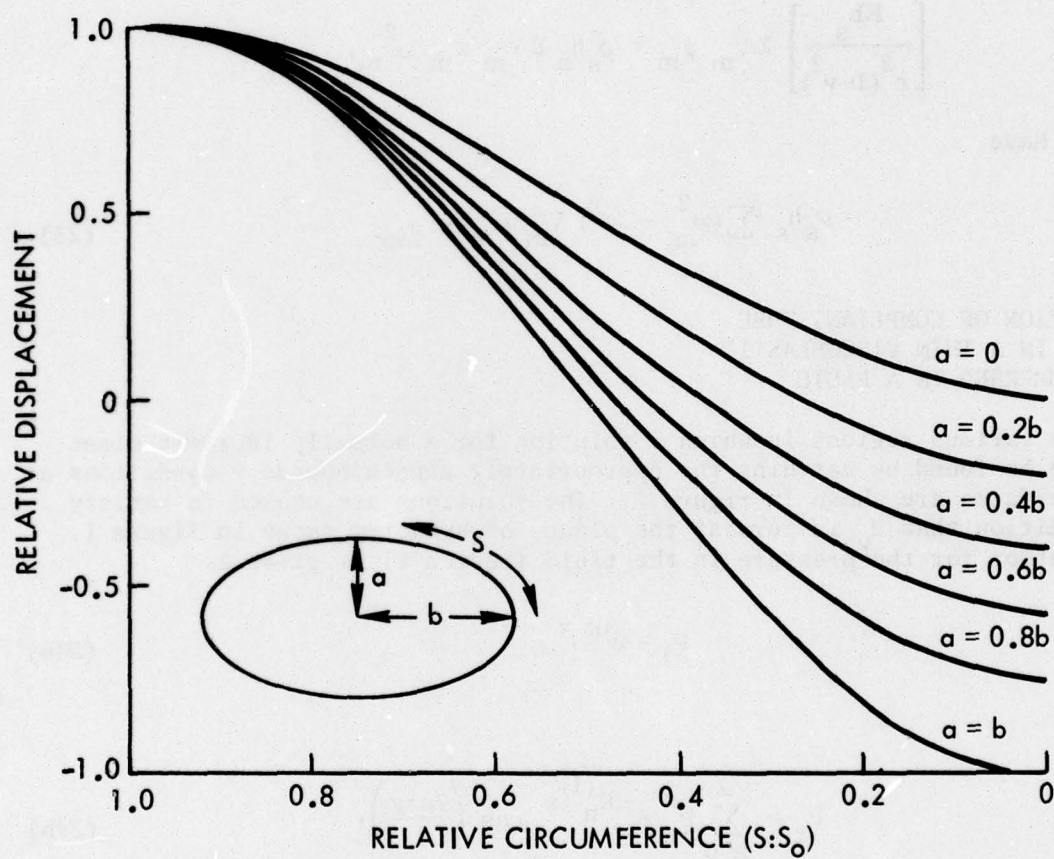


Figure 3. Fundamental Bending Waveform of an Elliptic Ring

If the tangential displacement is assumed zero and bending terms assumed negligible near the membrane resonances, then the resulting differential equation describing membrane motion is given by the reduced radial shell equation

$$\left[\frac{Eh_s}{r^2(1-\nu^2)} - \omega^2 \rho_s h_s \right] V = \sigma_{xx}, \quad (22)$$

where r is the local radius of curvature of the shell. Again using the normal modes defined for the homogeneous form of (22) such that

$$\left[\frac{Eh_s}{r^2(1-\nu^2)} \right] \Sigma V_m \psi_m = \rho_s h_s \Sigma V_m \psi_m \omega_m^2,$$

we then have

$$\rho_s h_s \Sigma (\omega_m^2 - \omega^2) V_m \psi_m = \sigma_{xx}. \quad (23)$$

DESCRIPTION OF COMPLIANT TUBE GRATING IN A THIN VISCOELASTIC LAYER IMMERSED IN A FLUID

The various regions in which a solution for a normally incident plane wave can be found by matching the appropriately chosen boundary conditions at the interfaces are shown in figure 1. The solutions are chosen to satisfy the condition that U_y is zero at the planes of symmetry shown in figure 1. The solution for the pressure in the field (region 1) is given as

$$P_i = e^{ik_o x} \quad (24a)$$

and

$$P_r = \sum_{n=0}^{\infty} P_n^r e^{-ik_n^{(1)} x} \cos\left(\frac{2n\pi y}{d}\right), \quad (24b)$$

where

$$\left(k_n^{(1)}\right)^2 = k_o^2 - \left(\frac{2\pi n}{d}\right)^2, \quad k_o = \frac{\omega}{c_o}. \quad (24c)$$

Here P_i is the incident plane wave pressure and P_r is the reflected wave. The wavenumber is k_0 in the fluid and d is the periodicity of the grating.

The viscoelastic layer is divided into three regions, as shown in figure 1. The scalar and vector potentials for the dilatational and shear waves, respectively, are given as

Region 2

$$\phi_2 = \sum_{n=0}^{\infty} \left\{ A_n^{(2)} e^{ik_{np}^{(2)}x} + B_n^{(2)} e^{-ik_{np}^{(2)}x} \right\} \cos \left(\frac{2n\pi y}{d} \right) \quad (25a)$$

$$A_2 = \sum_{n=1}^{\infty} \left\{ C_n^{(2)} e^{ik_{ns}^{(2)}x} + D_n^{(2)} e^{-ik_{ns}^{(2)}x} \right\} \sin \left(\frac{2n\pi y}{d} \right), \quad (25b)$$

where

$$k_{np}^{(2)} = \left[k_p^2 - \left(\frac{2\pi n}{d} \right)^2 \right]^{1/2}$$

$$k_{ns}^{(2)} = \left[k_s^2 - \left(\frac{2\pi n}{d} \right)^2 \right]^{1/2}.$$

Here k_p is the complex dilatational wavenumber and k_s is the complex shear wavenumber.

Region 3

The potentials in this region are chosen to satisfy the additional constraint that U_y is zero at $y = b$. In other words, for a normally incident dilatational wave, there is no translational motion of the compliant tubes in the y direction:

$$\phi_3 = \sum_{n=0}^{\infty} \left\{ A_n^{(3)} e^{ik_{np}^{(3)}x} + B_n^{(3)} e^{-ik_{np}^{(3)}x} \right\} \cos 2n\pi \left[(y - b)/l \right] \quad (26a)$$

$$A_3 = \sum_{n=0}^{\infty} \left\{ C_n^{(3)} e^{ik_{ns}^{(3)}x} + D_n^{(3)} e^{-ik_{ns}^{(3)}x} \right\} \sin 2n\pi \left[(y - b)/l \right],$$

where $\ell = d-2b$ and, to satisfy the wave equation,

$$\begin{aligned} k_{n_p}^{(3)} &= \left[k_p^2 - \left(\frac{2n\pi}{\ell} \right)^2 \right]^{1/2} \\ k_{n_s}^{(3)} &= \left[k_s^2 - \left(\frac{2n\pi}{\ell} \right)^2 \right]^{1/2}. \end{aligned} \quad (26b)$$

Region 4

$$\phi_4 = \sum_{n=0}^{\infty} \left\{ A_n^{(4)} e^{ik_{n_p}^{(4)} x} + B_n^{(4)} e^{-ik_{n_p}^{(4)} x} \right\} \cos \left(\frac{2n\pi y}{d} \right) \quad (27a)$$

$$A_4 = \sum_{n=1}^{\infty} \left\{ C_n^{(4)} e^{ik_{n_s}^{(4)} x} + D_n^{(4)} e^{-ik_{n_s}^{(4)} x} \right\} \sin \left(\frac{2n\pi y}{d} \right),$$

where

$$\begin{aligned} k_{n_p}^{(4)} &= \left[k_p^2 - \left(\frac{2n\pi}{d} \right)^2 \right]^{1/2} \\ k_{n_s}^{(4)} &= \left[k_s^2 - \left(\frac{2n\pi}{d} \right)^2 \right]^{1/2}. \end{aligned} \quad (27b)$$

Thus, the solutions in the viscoelastic layer and fluid are taken as the sum of propagating and evanescent plane waves whose direction is determined by the periodicity of the layer. Of course, the higher the order n of an evanescent wave, the more rapid the decay away from the grating.

The conditions in region 5 can be chosen as another fluid medium, an infinite impedance medium, or a finite elastic plate backed by a light or heavy fluid medium. The chosen backing then determines the boundary conditions at the interface between regions 4 and 5.

In the fluid region behind the layer, designated as region 5 in figure 1, the pressure is taken as a sum of outgoing plane waves with the periodicity of the grating, that is,

$$P_t = \sum_{n=0}^{\infty} P_n^t e^{ik_n^{(5)} x} \cos \left(\frac{2n\pi y}{d} \right), \quad (28a)$$

where, again

$$k_n^{(5)} = \left[k_0^2 - \left(\frac{2n\pi}{d} \right)^2 \right]^{1/2}. \quad (28b)$$

BOUNDARY CONDITIONS AND INFINITE SYSTEM OF EQUATIONS

The boundary conditions to be satisfied at the interfaces between the designated regions are as follows:

A. At $x = -t_1$

1. The tangential shear stress in the elastomer must be zero:

$$\sigma_{xy}^{(2)} = 0, \quad (29a)$$

which in terms of the potentials gives

$$\begin{aligned} & \sum_{n=0}^{\infty} \left\{ \left[\left(k_n^{(2)} \right)^2 - \left(\frac{2n\pi}{d} \right)^2 \right] \left(C_n^{(2)} e^{-ik_n^{(2)} t_1} + D_n^{(2)} e^{ik_n^{(2)} t_1} \right) \right. \\ & \left. + \frac{4ik_n^{(2)} n\pi}{d} \left(A_n^{(2)} e^{-ik_n^{(2)} t_1} - B_n^{(2)} e^{ik_n^{(2)} t_1} \right) \right\} \sin \left(\frac{2n\pi y}{d} \right) = 0. \end{aligned} \quad (29b)$$

2. The normal stress $\sigma_{xx}^{(2)}$ in the elastomer must be equal to the negative of the total pressure in the fluid

$$\sigma_{xx}^{(2)} = -P_T = -(P_i + P_r) \quad (30a)$$

or

$$\begin{aligned}
& \sum_{n=0}^{\infty} \left\{ \lambda k_p^2 + 2\mu \left(k_{np}^{(2)} \right)^2 \right\} \left(A_n^{(2)} e^{-ik_{np}^{(2)} t_1} + B_n^{(2)} e^{ik_{np}^{(2)} t_1} \right) \\
& - \frac{4\pi n}{d} \mu ik_{ns}^{(2)} \left(C_n^{(2)} e^{-ik_{ns}^{(2)} t_1} - D_n^{(2)} e^{ik_{ns}^{(2)} t_1} \right) \left\} \cos \left(\frac{2n\pi y}{d} \right) \\
& = e^{-ik_o t_1} + \sum_{n=0}^{\infty} P_n^r e^{ik_n^{(1)} t_1} \cos \left(\frac{2n\pi y}{d} \right). \quad (30b)
\end{aligned}$$

3. The normal deflection at the viscoelastic-fluid interface must be continuous,

$$u_x^{(2)} = \frac{1}{\omega^2 \rho} \frac{\partial P_T}{\partial x} \quad (31a)$$

or

$$\begin{aligned}
& \sum_{n=0}^{\infty} \left\{ ik_{np}^{(2)} \left(A_n^{(2)} e^{-ik_{np}^{(2)} t_1} - B_n^{(2)} e^{ik_{np}^{(2)} t_1} \right) \right. \\
& \left. + \frac{2\pi n}{d} \left(C_n^{(2)} e^{-ik_{ns}^{(2)} t_1} + D_n^{(2)} e^{ik_{ns}^{(2)} t_1} \right) \right\} \cos \left(\frac{2n\pi y}{d} \right) \\
& = \frac{1}{\omega^2 \rho} \left[ik_o e^{-ik_o t_1} - \sum_{n=0}^{\infty} ik_n^{(1)} P_n^r e^{ik_n^{(1)} t_1} \cos \left(\frac{2n\pi y}{d} \right) \right]. \quad (31b)
\end{aligned}$$

B. At $x = x_j = \pm a$

1. The normal displacements of the viscoelastic layer are continuous across the elastomer and equal to the compliant tube displacement at the tube walls:

$$u_x^{(j)} = u_x^{(3)} \quad |b| \leq y \leq |d/2| \quad j = 2, 4, \quad (32a)$$

which results in

$$\begin{aligned}
 & \sum_{n=0}^{\infty} \left\{ ik_{np}^{(j)} \left(A_n^{(j)} e^{ik_{np}^{(j)} x_j} - B_n^{(j)} e^{-ik_{np}^{(j)} x_j} \right) + \left(\frac{2n\pi}{d} \right) \left(C_n^{(j)} e^{ik_{ns}^{(j)} x_j} \right. \right. \\
 & \quad \left. \left. + D_n^{(j)} e^{-ik_{ns}^{(j)} x_j} \right) \right\} \cos \left(\frac{2\pi ny}{d} \right) \\
 & = \sum_{n=0}^{\infty} \left\{ ik_{np}^{(3)} \left(A_n^{(3)} e^{ik_{np}^{(3)} x_j} - B_n^{(3)} e^{-ik_{np}^{(3)} x_j} \right) \right. \\
 & \quad \left. + \left(\frac{2n\pi}{l} \right) \left(C_n^{(3)} e^{ik_{ns}^{(3)} x_j} + D_n^{(3)} e^{-ik_{ns}^{(3)} x_j} \right) \right\} \cos 2n\pi \left(\frac{y-b}{l} \right), \quad (32b)
 \end{aligned}$$

where $x_2 = -a$ and $x_4 = a$, and

$$u_x^{(j)} = \sum_t v_t^{(j)} \psi_t \quad y \leq |b| \quad (32c)$$

leads to

$$\begin{aligned}
 & \sum_{n=0}^{\infty} \left\{ ik_{np}^{(j)} \left(A_n^{(j)} e^{ik_{np}^{(j)} x_j} - B_n^{(j)} e^{-ik_{np}^{(j)} x_j} \right) \right. \\
 & \quad \left. + \left(\frac{2n\pi}{d} \right) \left(C_n^{(j)} e^{ik_{ns}^{(j)} x_j} + D_n^{(j)} e^{-ik_{ns}^{(j)} x_j} \right) \right\} \cos \left(\frac{2\pi ny}{d} \right) = \sum_t v_t^{(j)} \psi_t \\
 & \quad y \leq |b|. \quad (32d)
 \end{aligned}$$

The amplitudes of the tube displacement $v^{(j)}$ differ at most by a sign.

2. The equation of motion of the compliant tube is satisfied by the approximation

$$2 \rho_s h_s \sum_{t=1}^{\infty} \left(\omega_t^2 - \omega^2 \right) v_t \psi_t = \sigma_{xx}^{(2)} + \sigma_{xx}^{(4)} \quad y \leq |b| \quad (33a)$$

or

$$\begin{aligned}
& 2\rho_s h_s \sum_{t=1}^{\infty} \left(\omega_t^2 - \omega^2 \right) v_t \psi_t \\
&= - \sum_{n=0}^{\infty} \left\{ \left[\lambda k_p^2 + 2\mu \left(k_{np}^{(2)} \right)^2 \right] \left(A_n^{(2)} e^{-ik_{np}^{(2)} a} + B_n^{(2)} e^{ik_{np}^{(2)} a} \right) \right. \\
&\quad \left. + \frac{4\pi\mu i}{d} n k_{ns}^{(2)} \left[C_n^{(2)} e^{-ik_{ns}^{(2)} a} - D_n^{(2)} e^{ik_{ns}^{(2)} a} \right] \right\} \cos \left(\frac{2n\pi y}{d} \right) \\
&\pm \sum_{n=0}^{\infty} \left\{ \left[\lambda k_p^2 + 2\mu \left(k_{np}^{(4)} \right)^2 \right] \left(A_n^{(4)} e^{ik_{np}^{(4)} a} + B_n^{(4)} e^{-ik_{np}^{(4)} a} \right) \right. \\
&\quad \left. - \frac{4\pi\mu i}{d} n k_{ns}^{(4)} \left(C_n^{(4)} e^{ik_{ns}^{(4)} a} - D_n^{(4)} e^{-ik_{ns}^{(4)} a} \right) \right\} \cos \left(\frac{2n\pi y}{d} \right) , \quad (33b)
\end{aligned}$$

where t includes all modes symmetric to the x -axis.

For even-even modes the motion of the tube walls is symmetric with respect to the y -axis. For even-odd modes, the motion of the tube wall is antisymmetric with respect to the y -axis.

The normal stress is continuous across the elastomer:

$$\sigma_{xx}^{(j)} = \sigma_{xx}^{(3)} \quad |b| \leq y \leq \frac{d}{2} \quad j = 2, 4 \quad (33c)$$

or

$$\begin{aligned}
& \sum_{n=0}^{\infty} \left\{ \left[\lambda k_p^2 + 2\mu \left(k_{np}^{(j)} \right)^2 \right] \left(A_n^{(j)} e^{ik_{np}^{(j)} x_j} + B_n^{(j)} e^{-ik_{np}^{(j)} x_j} \right) \right. \\
&\quad \left. - \frac{4\pi n}{d} \mu i k_{ns}^{(j)} \left[C_n^{(j)} e^{ik_{ns}^{(j)} x_j} \right] \right\}
\end{aligned}$$

$$\begin{aligned}
& - D_n^{(j)} e^{-ik_n^{(j)} x_j} \} \cos \left(\frac{2n\pi y}{d} \right) = \sum_{n=0}^{\infty} \left\{ \left[\lambda k_p^2 + 2\mu_3 \left(k_n^{(3)} \right)^2 \right] \left[A_n^{(3)} e^{ik_n^{(3)} x_j} \right. \right. \\
& \left. \left. + B_n^{(3)} e^{-ik_n^{(3)} x_j} \right] - \frac{4n\pi}{l} \mu k_n^{(3)} \left[C_n^{(3)} e^{ik_n^{(3)} x_j} - D_n^{(3)} e^{-ik_n^{(3)} x_j} \right] \right\} \cos 2n\pi \left[\frac{(y-b)}{l} \right]. \quad (33d)
\end{aligned}$$

3. Tangential displacements are continuous across the elastomer and for bending mode, the displacements are equal to the inextensional tangential displacement across the tubes:

$$u_y^{(j)} = u_y^{(3)} \quad |b| \leq y \leq |d/2| \quad j = 2, 4 \quad (34a)$$

yields

$$\begin{aligned}
& \sum_{n=0}^{\infty} \left\{ \frac{2\pi n}{d} \left(A_n^{(j)} e^{ik_n^{(j)} x_j} + B_n^{(j)} e^{-ik_n^{(j)} x_j} \right) \right. \\
& \left. + ik_n^{(j)} \left(C_n^{(j)} e^{ik_n^{(j)} x_j} - D_n^{(j)} e^{-ik_n^{(j)} x_j} \right) \right\} \sin \left(\frac{2n\pi y}{d} \right) \\
& = \sum_{n=0}^{\infty} \left\{ \frac{2n\pi}{l} \left(A_n^{(3)} e^{ik_n^{(3)} x_j} + B_n^{(3)} e^{-ik_n^{(3)} x_j} \right) \right. \\
& \left. + ik_n^{(j)} \left(C_n^{(3)} e^{ik_n^{(3)} x_j} - D_n^{(3)} e^{-ik_n^{(3)} x_j} \right) \right\} \sin 2n\pi \left[\frac{(y-b)}{l} \right], \quad (34b)
\end{aligned}$$

and

$$u_y^{(j)} = r \frac{\partial V^{(j)}}{\partial y} = r \frac{\partial}{\partial y} \sum_t V_t^{(j)} \psi_t \quad y \leq |b| \quad (34c)$$

gives

$$\sum_{n=0}^{\infty} \left\{ -\frac{2\pi n}{d} \left(A_n^{(j)} e^{ik_{np}^{(j)} x_j} + B_n^{(j)} e^{-ik_{np}^{(j)} x_j} \right) - ik_{ns}^{(j)} \left(C_n^{(j)} e^{ik_{ns}^{(j)} x_j} - D_n^{(j)} e^{-ik_{ns}^{(j)} x_j} \right) \right\} \sin \left(\frac{2\pi n y}{d} \right) = r \sum_t V_t^{(j)} \frac{\partial \psi_t}{\partial y} \quad (34d)$$

For membrane modes, the tangential displacement of the compliant tube is assumed to be zero.

4. The tangential shear stress is continuous across the elastomer:

$$\sigma_{xy}^{(j)} = \sigma_{xy}^{(3)} \quad |b| < y < |d/2| \quad j = 2, 4 \quad (35a)$$

or

$$\begin{aligned} \mu \sum_{n=0}^{\infty} \left\{ 2i k_{np}^{(j)} \left(\frac{2\pi n}{d} \right) \left[A_n^{(j)} e^{ik_{np}^{(j)} x_j} - B_n^{(j)} e^{-ik_{np}^{(j)} x_j} \right] \right. \\ \left. + \left[\left(k_{ns}^{(j)} \right)^2 - \left(\frac{2\pi n}{d} \right)^2 \right] \left[C_n^{(j)} e^{ik_{ns}^{(j)} x_j} + D_n^{(j)} e^{-ik_{ns}^{(j)} x_j} \right] \right\} \sin \left(\frac{2\pi n y}{d} \right) \\ \mu \sum_{n=0}^{\infty} \left\{ 2i k_{np}^{(3)} \left(\frac{2\pi n}{\ell} \right) \left[A_n^{(3)} e^{ik_{np}^{(3)} x_j} - B_n^{(j)} e^{-ik_{np}^{(3)} x_j} \right] \right. \\ \left. + \left[\left(k_{ns}^{(3)} \right)^2 - \left(\frac{2\pi n}{\ell} \right)^2 \right] \left[C_n^{(3)} e^{ik_{ns}^{(3)} x_j} + D_n^{(3)} e^{-ik_{ns}^{(3)} x_j} \right] \right\} \sin 2\pi n \left[\frac{y-b}{\ell} \right] \end{aligned} \quad |b| \leq y \leq \frac{|d|}{2} \quad (35b)$$

and

$$\sigma_{xy}^{(j)} = 0 \quad y < |b| \quad (35c)$$

gives

$$\begin{aligned} & \mu \sum_{n=0}^{\infty} \left\{ 2ik_{n_p}^{(j)} \left(\frac{2\pi n}{d} \right) \left[A_n^{(j)} e^{ik_{n_p}^{(j)} x_j} - B_n^{(j)} e^{-ik_{n_p}^{(j)} x_j} \right] \right. \\ & \left. + \left[\left(k_{n_s}^{(j)} \right)^2 - \left(\frac{2\pi n}{d} \right)^2 \right] \left[C_n^{(j)} e^{ik_{n_s}^{(j)} x_j} + D_n^{(j)} e^{-ik_{n_s}^{(j)} x_j} \right] \right\} \sin \left(\frac{2\pi ny}{d} \right) = 0. \quad (35d) \end{aligned}$$

For thin walled compliant tubes, it is assumed that the tangential shearing stress does not produce a comparable stress in the tube walls.

C. At the elastic-fluid interface ($x = t_2$)

1. The tangential shear stress is zero:

$$\sigma_{xy}^{(4)} = 0 \quad (36a)$$

or in terms of the potentials

$$\begin{aligned} & \sum_{n=0}^{\infty} \left\{ \frac{4\pi n}{d} ik_{n_p}^{(4)} \left(A_n^{(4)} e^{ik_{n_p}^{(4)} t_3} - B_n^{(4)} e^{-ik_{n_p}^{(4)} t_3} \right) \right. \\ & \left. + \left[\left(k_{n_s}^{(4)} \right)^2 - \left(\frac{2\pi n}{d} \right)^2 \right] \left(C_n^{(4)} e^{ik_{n_s}^{(4)} t_3} + D_n^{(4)} e^{-ik_{n_s}^{(4)} t_3} \right) \right\} \sin \left(\frac{2\pi ny}{d} \right) = 0. \quad (36b) \end{aligned}$$

2. The normal stress in the plate is equated to the negative of the transmitted pressure in the fluid:

$$-P_t = \sigma_{xx}^{(4)} \quad (37a)$$

gives

$$\begin{aligned}
 & \sum_{n=0}^{\infty} P_n^t e^{ik_n^{(5)} t_3} \cos\left(\frac{2n\pi y}{d}\right) \\
 &= \sum_{n=0}^{\infty} \left\{ \left[\lambda \left(k_p^{(2)} \right)^2 + 2\mu \left(k_{np}^{(4)} \right)^2 \right] \left(A_n^{(4)} e^{ik_{np}^{(4)} t_3} + B_n^{(4)} e^{-ik_{np}^{(4)} t_3} \right) \right. \\
 & \quad \left. - \frac{4\pi n}{d} \mu ik_{ns}^{(4)} \left[C_n^{(4)} e^{ik_{ns}^{(4)} t_3} - D_n^{(4)} e^{-ik_{ns}^{(4)} t_3} \right] \right\} \cos\left(\frac{2n\pi y}{d}\right). \quad (37b)
 \end{aligned}$$

3. The normal deflection at the elastic interface is continuous

$$\frac{1}{\omega^2 \rho} \frac{\partial P_t}{\partial x} = u_x^{(4)} \quad (38a)$$

yields

$$\begin{aligned}
 & \frac{1}{\omega^2 \rho} \sum_{n=0}^{\infty} ik_n^{(5)} P_n^t \cos\left(\frac{2n\pi y}{d}\right) e^{ik_n^{(5)} t_3} \\
 &= \sum_{n=0}^{\infty} \left\{ ik_{np}^{(4)} \left(A_n^{(4)} e^{ik_{np}^{(4)} t_3} - B_n^{(4)} e^{-ik_{np}^{(4)} t_3} \right) \right. \\
 & \quad \left. + \left(\frac{2n\pi}{d} \right) \left(C_n^{(4)} e^{ik_{ns}^{(4)} t_3} + D_n^{(4)} e^{-ik_{ns}^{(4)} t_3} \right) \right\} \cos\left(\frac{2n\pi y}{d}\right). \quad (38b)
 \end{aligned}$$

The above equations are multiplied by, say, the orthogonal functions $\sin(2n\pi/d)y$ or $\cos(2n\pi/d)y$, and integrated over the typical grating spacing of 0 to $d/2$. The equations defined by (33a) are multiplied through by the appropriate deflection profile ψ_n and integrated about the tube in the interval $y \leq b$. For the comparisons of experimental data with calculations as shown in the next section, the analysis has been simplified. First, the tubes have been considered as infinitesimally thin (that is, $a \rightarrow 0$), and thus the width and contribution of region 3 shrinks to zero. Second, since only tightly packed compliant tube arrays are considered, a good approximate solution of closed form is obtained by satisfying the displacement equations over the entire grating spacing d at $x = 0$ and the stress equations only over the tube walls.¹⁷ As the grating spacing increases, full consideration must be given to the interstices between the tubes.

COMPARISON OF CALCULATIONS AND EXPERIMENTAL DATA

EXPERIMENTAL PROCEDURE

Comparisons of transmission through the layer of compliant tubes in a viscoelastic material were made with both 0.375 in. (9.525 mm) major axis Lexan plastic tubes and 0.925 in. (23.5 mm) major axis steel tubes. The plastic tubes had an a/b ratio of about 0.5 and the in-air fundamental flexural resonance was measured to be approximately 22 kHz. The static compressibility of the plastic tubes was 20 times greater than that of water. A cutaway plastic tube panel is shown in figure 4. The grating spacing in this example is about 0.45 in. (11 mm) and the panel is of dimensions 27 in. x 27 in. x 0.375 in. (0.69 m x 0.69 m x 9.525 mm). The 14 in. (0.35 m) long steel tubes had an a/b ratio of about 0.1, an in-air bending resonance of 7.0 kHz, and a static compressibility of about one hundred times of water. The adhesive bond between the steel tubes and the encapsulants was found to be stronger than that with the plastic tubes.

Measurements were initially made of the transmission through the grating. A standard receiving hydrophone was placed in close proximity to the center of the array on the panel's transmission side to measure the insertion loss. Insertion loss as used is defined as $20 \log_{10} |\text{Transmitted Pressure} / \text{Incident Pressure}|$. Insertion loss measurements were made to determine the effect of the elastomer on shifting the array resonance frequencies and decreasing the Q value (quality factor) of the resonances. The specific impedance ρc of the encapsulants in all cases was close to that of water. Here c is the longitudinal velocity of the material.

INSERTION LOSS

The effects of the viscoelastic encapsulant on the array resonances are considered in this section. In figure 5, a comparison of the measured and calculated insertion loss is made for the plastic tubes embedded in a low stiffness, low damping castable rubber, manufactured by B. F. Goodrich, that has both a density and longitudinal velocity close to that of water. The 0.5 in. (12.70 mm) thick panel had a 0.45 in. (11.50 mm) grating spacing. The fundamental bending mode and the first membrane mode are the most significant modes in the measured frequency range.

The shear modulus of the Goodrich material was determined to be 200 psi (1.38×10^6 n/m²) at 10 kHz with a corresponding loss factor of 0.2⁸. The loss factor is the ratio of the imaginary part of the complex modulus to the real part. These values were essentially constant in the temperature and frequency ranges of interest. Close agreement is found between the measured and calculated insertion loss in figure 5. The measured fundamental array bending mode resonance at about 18 kHz is similar to that of a single plastic tube in water. The measured insertion loss does not vary significantly from that of an unencapsulated array of similarly spaced compliant tubes found in reference 6, where at the array resonance, the unencapsulated panel acts as a dynamically soft reflector.

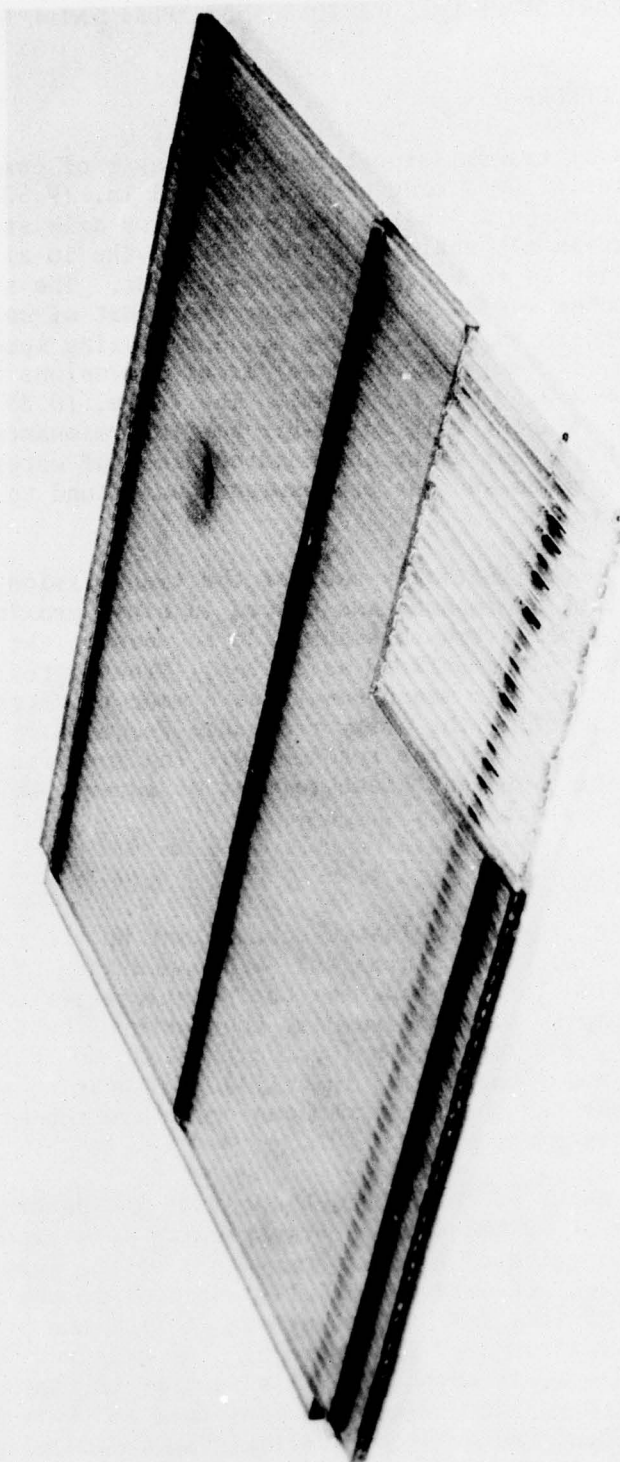


Figure 4. Plastic Tube Encapsulated in Polyurethane

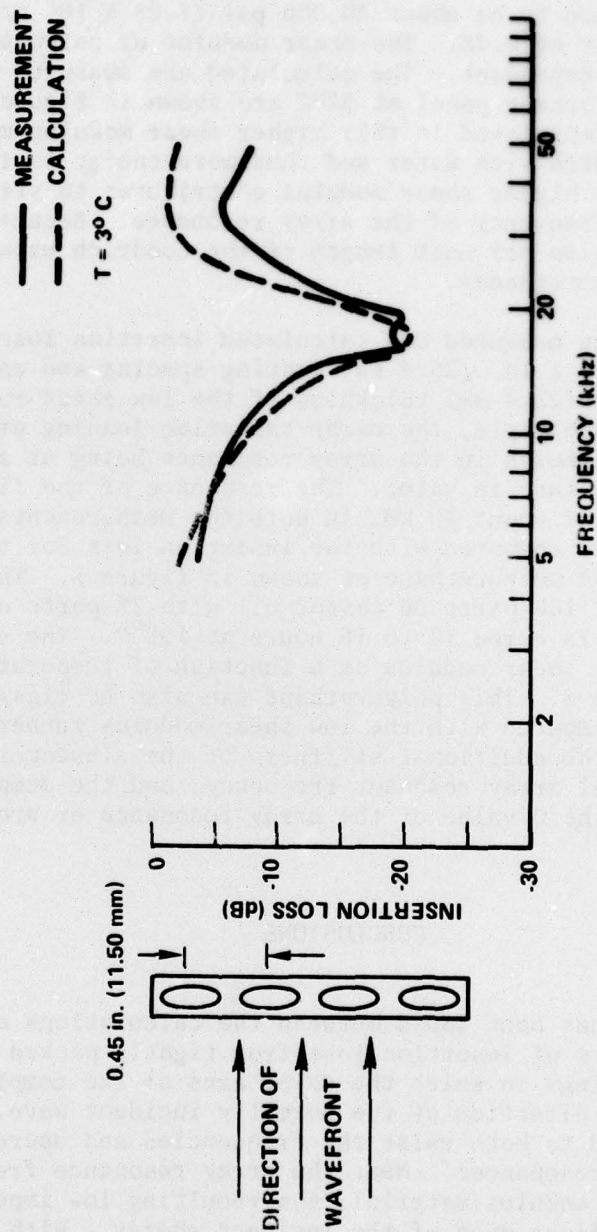


Figure 5. Comparison of Calculation and Measurement of Insertion Loss for 0.375 in. (9.52 mm) Lexan Plastic Tubes in a 0.45 in. (11.50 mm) Spaced Grating Encapsulated with a 0.5 in. (12.7 mm) Layer of Low Shear Modulus Rubber

The plastic tubes were then encapsulated in a 0.375 in. (9.5 mm) thick polyurethane panel. Measurements of the moduli of the polyurethane PRC-1534 could not be made because it contained a carcinogen and is no longer commercially available. A typical value of the shear modulus of the polyurethane PRC-1564 was determined to be about 20,000 psi (1.38×10^8 n/m²) with a corresponding loss factor of 0.48. The shear modulus of polyurethane is, however, strongly temperature dependent. The calculated and measured insertion loss curves for the polyurethane panel at 22°C are shown in figure 6. The closely spaced tube array encapsulated in this higher shear modulus material provides a better impedance match with water and thus more energy is transmitted through the panel. Also, the higher shear modulus contributes to stiffness loading which increases the frequency of the array resonance. Because of its low shear modulus, the attenuation per unit length of the Goodrich material is greater than that of the polyurethanes.

Comparison of the measured and calculated insertion loss for the steel compliant tubes with a 1 in. (25.4 mm) grating spacing and encapsulated in approximately a 1 in. (25.4 mm) thickness of the low shear rubber is shown in figure 7. In this example, the array radiation loading of the closely spaced tubes alone, results in the array resonance being at a higher frequency than that of a single tube in water. The resonance of the first harmonic even bending mode is seen at about 40 kHz in both the measurements and calculations. These curves are to be compared with the insertion loss for the same array encapsulated in NUSC-A polyurethane as shown in figure 8. The polyurethane is a castable mixture of 100 parts DB castor oil with 28 parts of tolylene diisocyanate; the mixture is cured 12 to 18 hours at 158°F. The specific gravity is 1.03. The complex shear modulus as a function of temperature and pressure is given in reference 8. This polyurethane can also be classified as a stiff-lossy polymer when compared with the low shear modulus rubber compound. As seen from figure 8, the additional stiffness of the elastomer significantly raises the fundamental array resonant frequency, and the damping due to the elastomer decreases the Q value of the array resonance or broadens the insertion loss resonance.

CONCLUSIONS

Good agreement has been found between the calculations of the analytical model and measurements of insertion loss from tightly packed compliant tubes in viscoelastic coatings in which the major axes of the compliant tubes are perpendicular to the direction of the normally incident wave. High shear modulus polymers tend to both raise the frequencies and decrease the quality factor of the array resonances. Near the array resonance frequencies of the tubes in a low shear modulus material, the resulting low impedance of these coatings tends to reflect much of the incident energy. With increased stiffness of the encapsulant, more energy is transmitted through the layer at the array resonance. In general, the effects of a high shear modulus polymer are temperature sensitive.

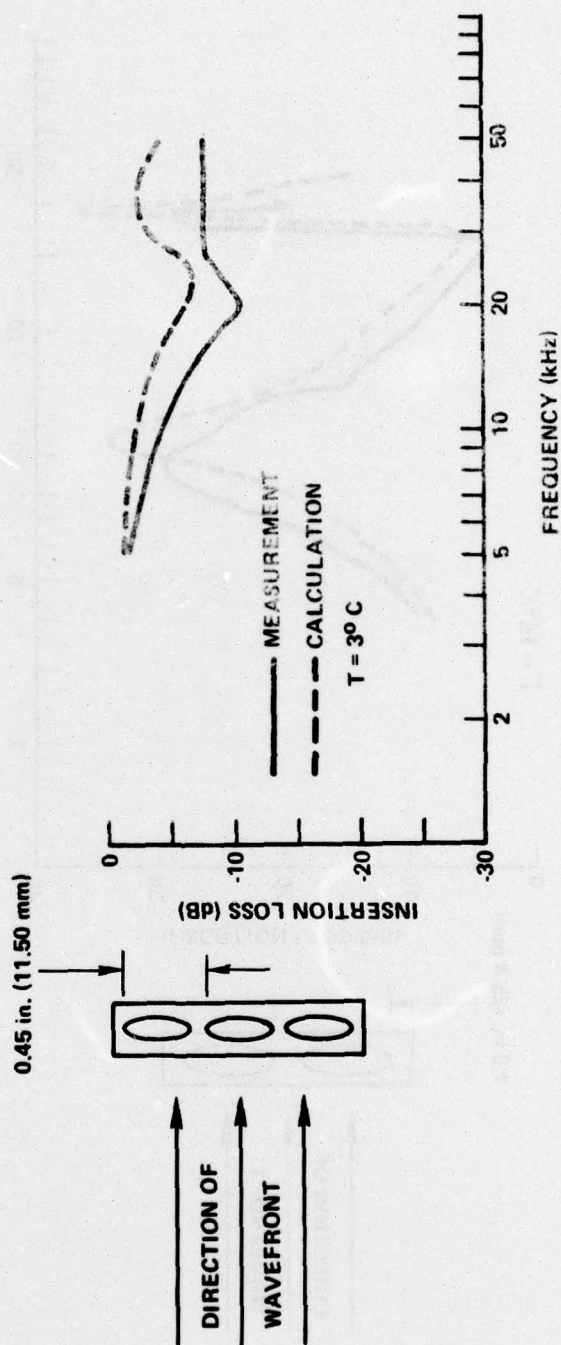


Figure 6. Comparison of Calculation and Measurement of Insertion Loss for 0.375 in. (9.52 mm) Lexan Plastic Tubes in a 0.45 in. (11.50 mm) Spaced Grating Encapsulated with a 0.5 in. (12.7 mm) Layer of Polyurethane

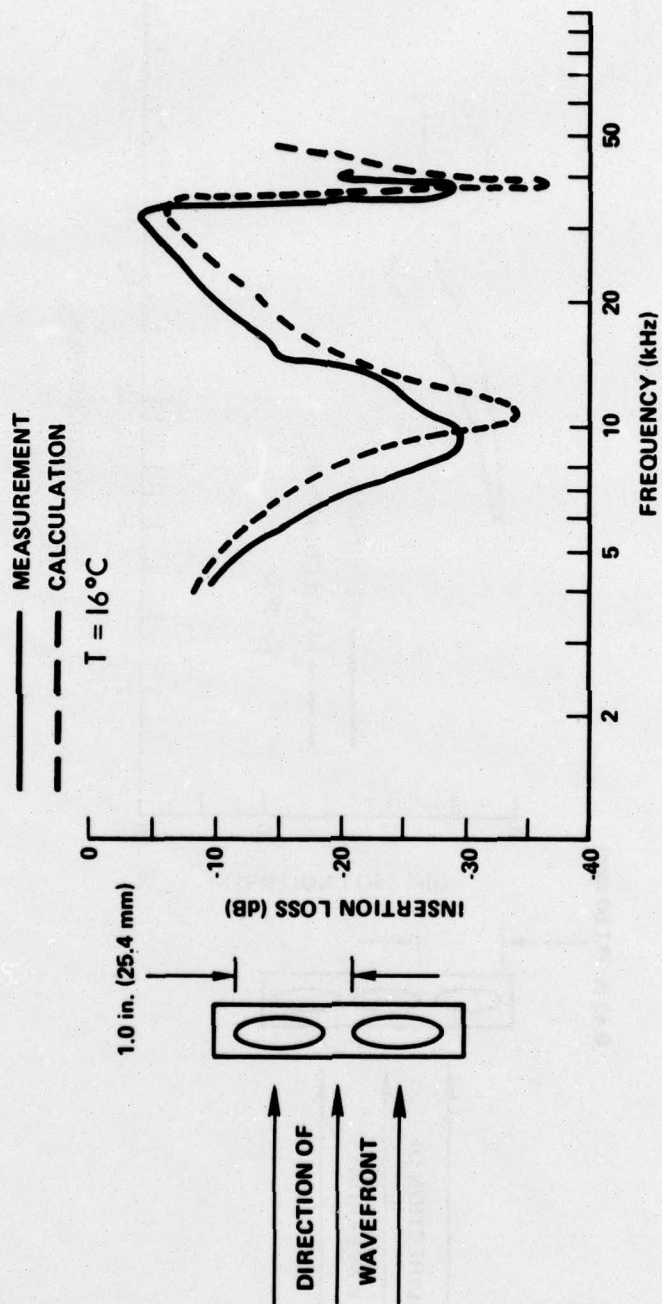


Figure 7. Comparison of Calculation and Measurement of Insertion Loss for 0.925 in. (23.50 mm) Steel Compliant Tubes in a 1 in. (25.4 mm) Spaced Grating Encapsulated with a 1 in. (25.4 mm) Thick Layer of Low Shear Modulus Rubber

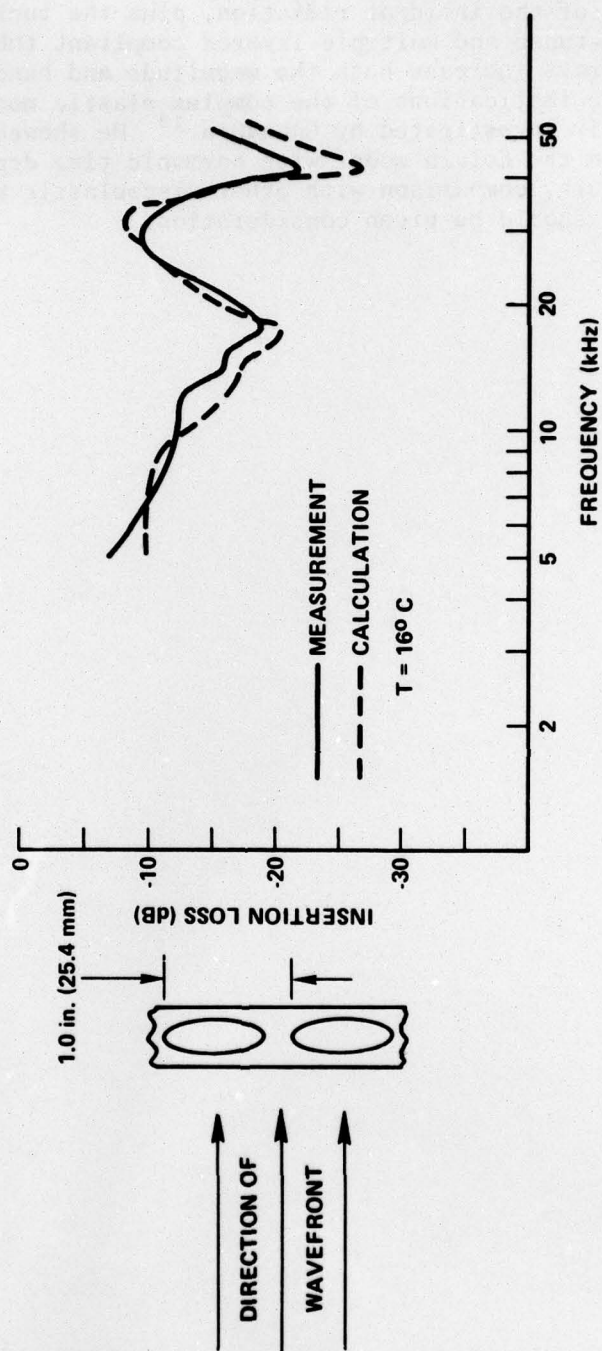


Figure 8. Comparison of Calculation and Measurement of Insertion Loss for 0.925 in. (23.5 mm) Steel Compliant Tubes in a 1 in. (25.4 mm) Spaced Grating Encapsulated with a 1 in. (25.4 mm) Thick Layer of Polyurethane

Further improvements in the model should include generalizations of tube orientation and angle of the incident radiation, plus the inclusion of the analysis of staggered-tuned and multiple-layered compliant tube arrays. These more complex arrays increase both the magnitude and bandwidth of insertion loss.¹⁸ The implications of the complex elastic moduli treatment have been recently investigated by Gaunaud.¹⁹ He showed that this model is equivalent to the Kelvin model with harmonic time dependence assumed. In future work, comparison with other viscoelastic models, such as the Maxwell model, should be given consideration.

REFERENCES

1. W. J. Toulis, "Acoustic Refraction and Scattering with Compliant Elements," Journal of the Acoustical Society of America, vol. 29, no. 29, pp. 1021-1033, 1957.
2. J. J. Libuha, R. P. Radlinski, and G. A. Brigham, "Scattering from Large Plane Gratings of Compliant Tubes," NUSC Technical Memorandum TD12-434-75, 8 December 1975.
3. C. H. Sherman, "Compliant Tubes for Reflectors: A Design Method," NUSL Memorandum Serial No. 1150-28, 6 June 1958.
4. G. A. Brigham, Scattering of Plane Waves by an Infinite Grating of Elliptic Cylindrical Shells, Technical Report B-103-73, Gerald Brigham and Associates, Inc., 1973.
5. R. P. Radlinski, "Modeling Predictions of Scattering from Planar Compliant Tube Arrays," NUSC Technical Memorandum TD12-40-74, 22 February 1974.
6. G. A. Brigham, J. J. Libuha, and R. P. Radlinski, Scattering from Large Planar Grating of Compliant Cylindrical Shells, NUSC Technical Report 5327, 27 April 1976.
7. G. A. Brigham, Scattering of Plane Longitudinal Waves by an Infinite Grating of Elliptical Cylindrical Shells Embedded in an Elastomer, Technical Report B-107-74, Gerald A. Brigham and Associates, Inc., 23 August 1974.
8. R. E. Strakna, Determination of the Complex Young's Modulus of Selected Polymers Using the WLF Transformation, NUSC Technical Report 5251, 10 October 1975.
9. J. R. Moriarty, "Acoustic Properties of Polymer and Composite Materials," NUSC Technical Memorandum SB322-4300-74, 29 July 1974.
10. H. F. Cooper, "Reflection and Transmission of Oblique Plane Waves at a Plane Interface Between Viscoelastic Media," Journal of the Acoustical Society of America, vol. 42, no. 5, pp. 1064-1069, 1967.
11. H. F. Cooper and E. L. Reiss, "Reflection of Plane Viscoelastic Waves for Plane Boundaries," Journal of the Acoustical Society of America, vol. 39, no. 6, pp. 1133-1138, 1960.
12. P. W. Buchen, "Plane Waves in Linear Viscoelastic Media," Geophysics Journal of the Royal Astrological Society, vol 23, pp. 531-592, 1971.
13. R. D. Borchardt, "Energy and Plane Waves in Linear Viscoelastic Media," Journal of Geophysical Research, vol. 78, no. 14, pp. 2442-2453, 1973.

14. R. D. Borchardt, "Rayleigh-Type Surface Waves on a Linear Viscoelastic Half-Space," Journal of the Acoustical Society of America, vol. 55, no. 1, pp. 13-15, 1974.
15. G. A. Brigham, "In-Plane Free Vibrations of Tapered Oval Rings," Journal of the Acoustical Society of America, vol. 54, no. 2, pp. 451-460, 1973.
16. G. A. Brigham, Lumped-Parameter Analysis of the Class IV (Oval) Flex-tensional Transducer, NUSC Technical Report 4463, 15 August 1973.
17. G. A. Brigham, Modeling the Acoustic Transmission of Compliant Tube Gratings in a Thin Elastomer Blanket, Technical Report B-108-74, G. A. Brigham and Associates, Inc., 30 August 1974.
18. Gerald A. Brigham, J. J. Libuha, and Ronald P. Radlinski, "Analysis of Scattering from Large Planar Gratings of Compliant Cylindrical Shells," Journal of the Acoustical Society of America, vol. 61, no. 1, pp. 48-59, 1977.
19. G. C. Gaunard, Methods for Solving the Viscoelasticity Equations for Cylinder and Sphere Problems, NSWC/WOL/TR-76-20, 22 March 1976.

INITIAL DISTRIBUTION LIST

Addressee	No. of Copies
ASN(R&D)	1
ONR, Code 102-OS, 412-8, 412-3, 483, 410,	6
CNO, OP-02, -090, -20, -201, -953	6
CNM, MAT-00, -03, -03B, -03L, -03L4, -0302, -0351, -0352, 032,	11
ASW-14, -23	1
NAVSHIPRANDCEN, ANNA	1
NAVSHIPRANDCEN, CARD	1
NRL, Underwater Sound Reference Division	2
NAVELECSYSCOMHQ, Code 03	1
NAVSEA, SEA-03C, -032, -034, -035, -037, -0552, -06H1(2)	
-06H1-1, 06H1-2, -06H1-3, -06H2 (E. Landers)(2),	
-06H4, -06H5, -060, -09G3(4), -0660C, -0660D, -662	23
NAVAIRDEVCCEN	1
NAVWPNSCEN	1
DTNSRDC, Code 1960 (W. Reader, J. Goodman), (R. Biancardi)	4
NAVCOASTSYSLAB	1
NAVSURFWPNCEN (G. C. Gaunaurd)	2
NAVUSEACEN	1
NAVSHIPYD PUGET	1
NAVSHIPYD MARE	1
NAVSEC, SEC-6034	1
NAVTRPSTA	1
NAVSUBSCOL	1
NAVPGSCOL	1
NAVWARCOL	1
APL/UW, SEATTLE	1
ARL/PENN STATE, STATE COLLEGE	1
DDC, ALEXANDRIA	12
IRIA	1
MARINE PHYSICAL LAB, SCRIPPS	1
ENV RES LAB (NOAA/ERL)	1
NATIONAL RESEARCH COUNCIL (COMMITTEE UNDERSEA WARFARE)	1
WEAPON SYSTEM EVALUATION GROUP	1
WOODS HOLE OCEANOGRAPHIC INSTITUTION	1
Cambridge Collaborative, Cambridge (Dr. J. Moore)	1
SACLANT RESEARCH CENTRE	1